J Electroceram (2007) 19:349–355
DOI 10.1007/s10832-007-9051-4

Energy harvesting using piezoelectric materials: Case of random vibrations

Elie Lefeuvre · Adrien Badel · Claude Richard · Daniel Guyomar

Received: 24 February 2006 / Accepted: 21 August 2006 / Published online: 16 February 2007

Abstract A dramatic consumption reduction of integrated circuits related to the development of mobile electronic devices has been reached over the past years, enabling the use of ambient energy instead of batteries. The focus is here on the transformation of ambient mechanical vibrations into electrical energy. This paper compares the performances of a vibration-powered electrical generator using PZT piezoelectric ceramics associated to two different power conditioning circuits. A new approach of the piezoelectric power conversion based on a nonlinear voltage processing is presented and implemented using a particular circuit. Theoretical predictions and experimental results show that the new technique may increase the power harvested by a factor up to 4 compared to the Standard technique. The power optimization problem is in particular examined in the case of broadband, random vibrations.

Keywords Energy harvesting · Energy scavenging · Power optimization · Piezoelectric materials · Vibration

1 Introduction

The use of piezoelectric materials for converting mechanical energy into electrical energy is not a recent idea. But in practice piezoelectric electrical generators remain limited to very low power domain, usually in the milliwatt range or below. This is mainly due to mechanical properties of piezoelectric materials: they accept very large stresses but their strains are very small, making difficult the use of large material quantities. Another point concerns the high mechanical frequencies necessary to effectively use these materials: ambient mechanical vibrations usually remain in the range 0.1–1 kHz, whereas piezoelectric materials may work up to hundreds of kilohertz. Nevertheless, recent development of wearable electronics and wireless systems combined with dramatic progresses in the domain of ultra-low power electronics stimulated extensive researches on the use of piezoelectric materials for converting ambient mechanical energy into electrical energy [8, 9]. Arms et al. have demonstrated a wireless sensing node including a microprocessor, on-board memory, strain sensing gauge, sensor signal conditioning, and 2.4 Ghz IEEE 802.15.4 radio transceiver with extremely low average consumption: the whole system consumes 900 μW for a 10 Hz sampling frequency and 90 μW only for a 1 Hz sampling frequency [1], making possible the use of a piezoelectric device as the power generator of the autonomous sensing node.

Size minimization and effective use of the active material require a careful optimisation of vibration-powered Piezoelectric Electrical Generators (PEGs). In particular, these generators exhibit large effectiveness variations, depending on the electrical properties of the circuit connected to terminal electrodes of their piezoelectric elements. In this field, several optimization approaches have been proposed. Previous works described a quasi-linear resistance adaptation approach [6, 7], so called "Standard" optimization technique. Other approaches based on particular non-linear processing of the piezoelectric output voltage [2–5] demonstrated their ability to significantly increase the energy converted by piezoelectric materials, leading in certain cases to an augmentation of the PEGs output power by a factor above 10. One of these new techniques has moreover another interesting property:

E. Lefeuvre (✉) · A. Badel · C. Richard · D. Guyomar
LGEF Laboratory, INSA de Lyon, 8 rue de la Physique,
69621 Villeurbanne, France
e-mail: elie.lefeuvre@insa-lyon.fr

it intrinsically solves the problem of the load resistance adaptation [4, 5]. Indeed, using the Standard technique it may be practically difficult to achieve the right tuning of the load impedance in the case of broadband, random vibrations. And, in practice, ambient vibrations are neither of constant amplitude nor on a single frequency.

Both optimization techniques are presented and theoretically compared in the case of harmonic mechanical vibrations. Experimental harmonic behaviour of a multimodal PEG on its first three modes is presented. Then, effectiveness of the self-tuned optimization technique, so called "Synchronous Electric Charge Extraction" (SECE), is compared to the Standard technique with various broadband, random vibrations.

2 PEG structures

A PEG is usually composed of a mechanical part, whose role is to collect ambient mechanical vibration and subject the active material to stress and strain variations. Through its electromechanical coupling property, the piezoelectric material converts the mechanical energy resulting from stress and strain variations into electrical energy. In open circuit configuration, an alternating voltage thus develops across the terminal electrodes of the active material.

Most of the electric loads, for instance electronic components, are powered with DC voltage. That's why an electronic power conversion interface is usually placed between the terminal electrodes of the active material and the power supply inputs of the electric load (Fig. 1). This power conversion interface can be as simple as a diode rectifier associated to a voltage smoothing capacitor. However, from the electrical side, a piezoelectric element can be basically modelled by a current source in parallel with a capacitor (or a voltage source in series with the same capacitor) and the search for a maximization of the power leads naturally to a linear impedance adaptation approach [6, 7]. From its power supply inputs, the electric load may be considered as equivalent to a resistor, or a voltage source if a battery is used as energy storage. A maximum of the power converted by the piezoelectric material can be tracked by controlling the piezoelectric output current respectively with the variations of ambient vibrations. The power conversion interface may thus play a key role in PEGs power optimization.

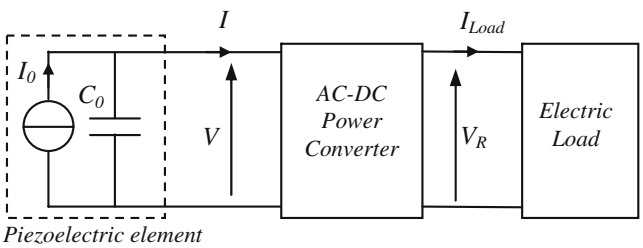

Fig. 1 PEG electrical circuit

2.1 Mechanical part

Many mechanical structures have been envisioned to transmit environmental vibrations to active material. These structures can be classified into two main categories. The first category includes the structures sensitive to ambient mechanical accelerations. In this case, the structures are mechanical resonators having only one or several resonance frequencies. Effective transmission of surrounding vibrations to piezoelectric material depends on the matching between the resonance frequencies and the environmental frequencies. Because of the mechanical filtering, only a few specific frequencies must be considered for power optimization.

In the second category, PEGs mechanical structures directly use strain variations of the vibrating host structure and adapt it to active material. Instead of being limited to specific resonance frequencies, the frequency spectrum of mechanical strain/stress transmitted to the active material is a function of the strain variations existing in the host structure. The frequency spectrum may be truly broadband for this PEG category. Thus, random environmental vibrations will not have the same effect and will not be harvested in the same way for both structures categories.

2.2 Piezoelectric material

Choice among many available piezoelectric materials is mainly guided by the need of an important intrinsic electromechanical coupling, leading to a high power density and facilitating PEG miniaturization. Material stiffness and maximum stress characteristics help in the design of the mechanical part. The material mechanical quality factor may also be also a parameter to consider, more particularly for power conversion in high frequencies. The output voltage range needed and the available stress levels help to determine the inter-electrodes distance. Most common geometries are plates or disks, with various possibilities for electrodes disposition [9].

Energy conversion analysis can be derived from piezoelectric equations (1), where *{T}*, *{S}*, *{E}* and *{D}* are respectively the stress, the strain, the electric field and the electrical induction. The piezoelectric material physical properties are the elastic stiffness determined at constant electric field $[c^E]$, the piezoelectric stress *[e]* and the permittivity at constant strain $[\varepsilon^S]$. *'t'* refers to matrix transpose.

$$\begin{Bmatrix} T \\ D \end{Bmatrix} = \begin{bmatrix} c^E & -e \\ e^t & \varepsilon^s \end{bmatrix} \begin{Bmatrix} S \\ E \end{Bmatrix} \quad (1)$$

In the case of vibration wavelengths much larger than the considered piezoelectric insert's dimensions, this insert

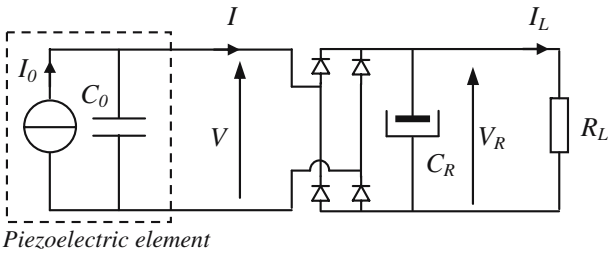

Fig. 2 PEG using a diode bridge as an AC–DC power conversion interface

can be roughly modeled as a single dimensions system. Its electromechanical behavior can be expressed as a function of an equivalent displacement u, the piezoelectric voltage V, an equivalent mechanical force F_p and the outgoing electric charge Q, as shown in Eqs. 2. In theses equations, C_0 is the clamped capacitance, α represents the force factor (Newton per Volt), and K^E is the equivalent short-circuit stiffness of the piezoelectric insert. In the simplest cases, these three factors may be analytically derived from the material piezoelectric properties (1) and from the mechanical setup characteristics. Their numerical values can be calculated using a finite element model. They may also be measured on an experimental prototype.

$$\begin{cases} F_P = K^E \cdot u + \alpha \cdot V \\ Q = \alpha \cdot u - C_0 \cdot V \end{cases} \tag{2}$$

From the electrical point of view, the second equation (2) shows that the piezoelectric insert used in a PEG can be basically modeled by a current source controlled by the mechanical velocity $I_0 = \alpha \cdot \dot{u}$, in parallel with a capacitor C_0.

2.3 Power optimization interfaces

As stated in the beginning of Section 2, the AC–DC power converter represented on Fig. 1 may be used as power optimization. The Standard power optimization technique can be analyzed in considering the structure represented on Fig. 2, where the AC–DC power converter in composed of a diode rectifier and a smoothing capacitor C_R. The electric load is modeled by an equivalent resistor R_L. The

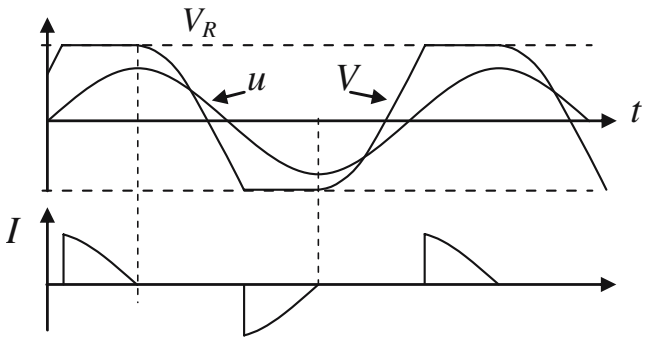

Fig. 3 Mechanical displacement, piezoelectric voltage and current with the standard technique

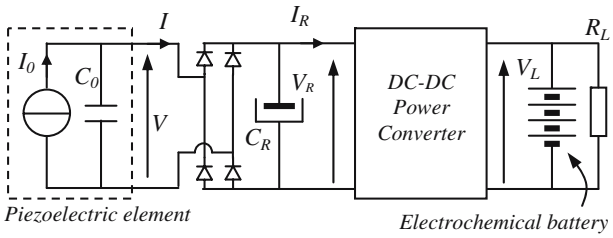

Fig. 4 Circuit for implementation of the standard technique including a DC–DC power converter for power optimization

corresponding mechanical displacement, piezoelectric voltage and current waveforms are represented on Fig. 3. For this configuration, Eq. 3 gives the average electrical power produced by the PEG in the case of harmonic mechanical displacement u, whose amplitude and angular frequency are U_M and ω [5].

$$P = R_L \frac{(\alpha \cdot \omega \cdot U_M)^2}{\left(R_L C_0 \omega + \frac{\pi}{2}\right)^2} \tag{3}$$

A thorough analysis would require a model of the mechanical part of the considered PEG. Indeed, the mechanical energy converted by the active material may induce more or less important variations on the mechanical displacement u and thus on the generated current I_0. Considering that energy harvesting only induces a weak mechanical damping, the PEG power reaches a maximum P_{Max} for a particular value R_{Lopt} of the load equivalent resistance defined in Eq. 4.

$$P_{max} = \frac{\alpha^2 \omega}{2\pi C_0} U_M^2, \quad R_{Lopt} = \frac{\pi}{2 C_0 \omega} \tag{4}$$

Thus, in the case of harmonic vibrations, the PEG power optimisation can be summarized as a tuning between the displacement amplitude U_M and the load resistance R_L. In an actual PEG, the load may include an energy storage cell such as a large capacitor or an electrochemical battery to overcome variations of ambient vibrations. In this case, a constant load voltage V_R is considered instead of the load equivalent resistance R_L. The PEG power expression is then given by Eq. 5. The PEG maximum power P_{Max} is the same as in Eq. 4, but it is expressed in Eq. 6 as a function of the optimal load voltage V_{Ropt} related to the displacement amplitude.

Maximization of the PEG power whatever the mechanical displacement amplitude requires an additional interface

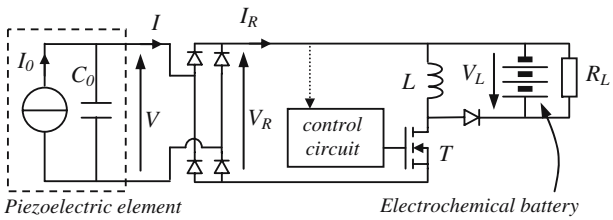

Fig. 5 Synchronous electric charge extraction circuit

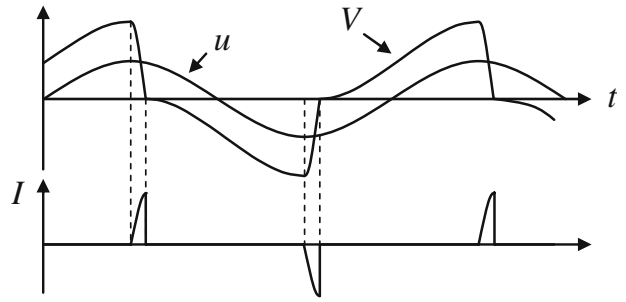

Fig. 6 Displacement, piezoelectric voltage and current with the SECE technique

shown on Fig. 4, allowing the permanent tuning of the rectified voltage V_R to the optimal value. This interface, a DC-to-DC power converter, must induce as few power losses as possible. In this domain, switching-mode power converters are known for their high efficiency. The development of portable electronic devices led to important technological progress of low-power switching-mode power converters: their efficiency reaches now currently the region of 90–95%.

This first power optimization approach may be qualified of "quasi-linear," although the diode rectifier bridge and the smoothing capacitor induce a distortion on the piezoelectric voltage V. But previous works showed that some DC–DC power converters may also be used to increase in a particular way the piezoelectric voltage non-linearities [4, 5]. As a result, the energy conversion capability of the active material is greatly enhanced. Another advantage of this nonlinear technique, so called "Synchronous Electric Charge Extraction" (SECE), is its self-optimization property: the PEG power remains at maximum whatever the load voltage or equivalent resistance.

$$P = \frac{2C_0\omega}{\pi} V_R \left(\frac{\alpha}{C_0} U_M - V_R \right) \tag{5}$$

$$P_{Max} = \frac{2C_0\omega}{\pi} \cdot V_{Ropt}^2 \quad V_{Ropt} = \frac{\alpha}{2C_0} U_M \tag{6}$$

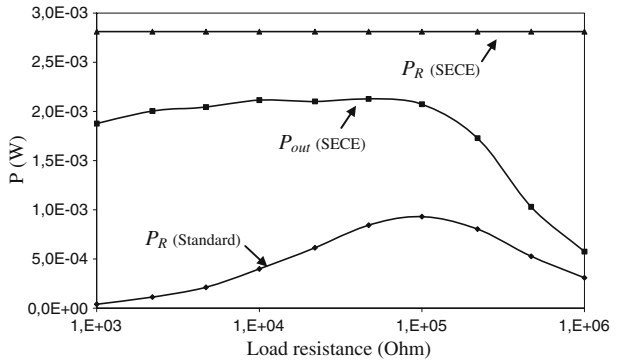

Fig. 7 Powers as a function of the load resistance for the first vibration mode (56 Hz)

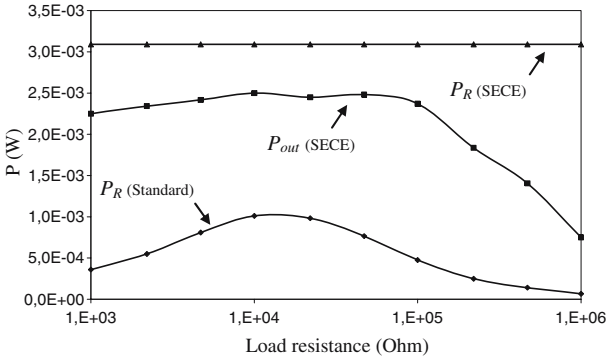

Fig. 8 Powers as a function of the load resistance for the second vibration mode (334 Hz)

The SECE technique is implemented with the buck–boost power converter structure represented on Fig. 5, with a particular control: the transistor T is turned ON each time the rectified voltage V_R reaches a maximum, and it is turned OFF each time V_R reaches zero. So, at each triggering time, the power converter removes completely the electric charge stored on the piezoelectric element electrodes and transmits the corresponding energy to the load, through the inductor L. The inductor value is chosen in considering the piezoelectric element capacitance, so that the time needed to extract the electric charge is much shorter than the vibration period. The corresponding mechanical displacement, piezoelectric voltage and current waveforms are presented on Fig. 6. The average power converted by the active material is given in Eq. 7. According to Eqs. 4 and 7, with the same mechanical displacement amplitude the power converted is theoretically four times greater using the SECE technique than with the Standard technique.

$$P = \frac{2\alpha^2\omega}{\pi C_0} U_M^2 \tag{7}$$

3 Multimodal vibrations

Starting from the power optimization analysis in the case of harmonic mechanical vibrations presented in Section 2.3 it

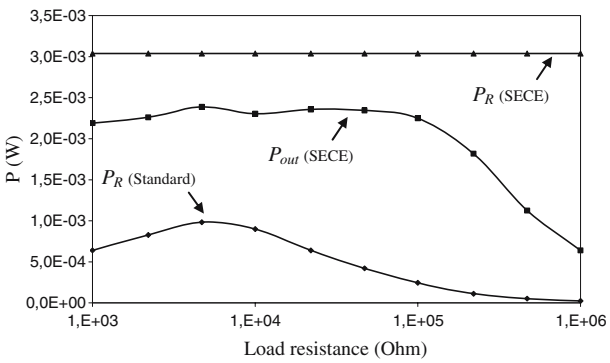

Fig. 9 Powers as a function of the load resistance for the third vibration mode (915 Hz)

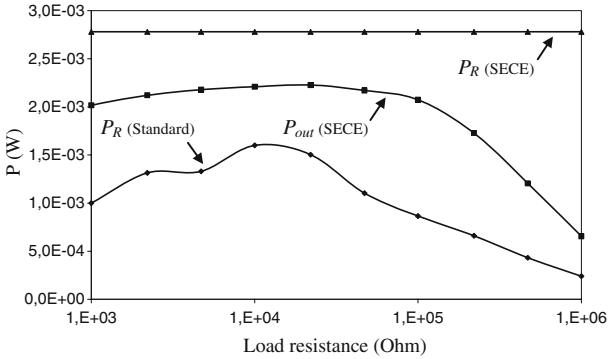

Fig. 10 Powers as a function of the load resistance, three modes mixed

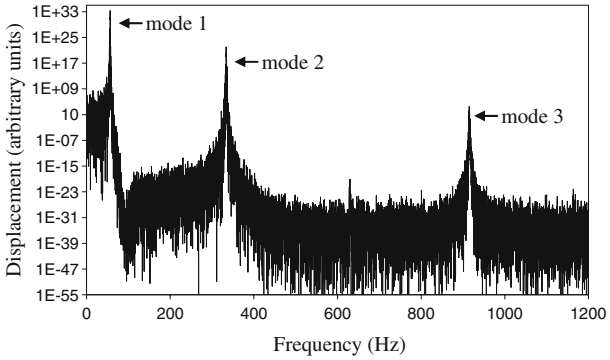

Fig. 12 Mechanical displacement spectrum, PEG driven by a random force in the 10 Hz–2 kHz band

is possible to consider the PEG behavior in the case of steady-state, multimodal mechanical vibrations. The mechanical part of the considered multimodal PEG is a cantilever steel beam, whose three first bending modes frequencies are respectively 56, 334 and 915 Hz. The beam vibrations are driven by an electromagnet controlled by a function generator through a power amplifier. The piezoelectric material used is a P1-89 PZT ceramic (Saint-Gobain, QS France). This piezoelectric insert is composed of six $9\times28\times0.3$ mm^3 plates bonded near the clamped edge. The global capacitance value of C_0 is 41.8 nF. A second identical piezoelectric insert bonded on the opposite side of the cantilever beam is used as mechanical displacement transducer. The Standard power optimization circuit is not completely implemented: it is composed of a diode bridge and a 2.2 μF smoothing capacitor C_R in parallel with a variable resistor R_L. The SECE circuit is implemented as described on Fig. 5, but the electrochemical battery is replaced by a 2.2 μF capacitor. The control circuitry of this second optimization interface is powered by an external power supply.

First, an experimental analysis of the PEG behavior is achieved for each of the mechanical modes separately. For each frequency, the displacement amplitude is tuned in order to reach 1 mW maximum power in the case of the Standard technique. Experimental results presented on Figs. 7, 8 and 9 confirm that maximum power of the Standard technique is reached with nearly the optimal load resistance values defined in Eq. 4, which are respectively 106, 18 and 6.5 kΩ. Plots referred as "P_R (standard)" and "P_R (SECE)" represent the rectifier bridge average power output respectively with the Standard circuit and the SECE circuit. Plots referred as "P_{out} (SECE)" represent the average power consumed by the terminal load resistance R_L of the SECE circuit. According to Eqs. 4 and 6, the SECE technique should theoretically harvest 4 times more power than the Standard technique, but measurements show that the power is only increased by a factor 3. Difference between theoretical and experimental power gains are in particular due to the piezoelectric material leakage resistance which is not taken into account in the model.

Input power of the SECE circuit ("P_R (SECE)") confirms to be constant whatever the load resistance, whereas output power ("P_{out} (SECE)") decreases for high values of the load resistance because of the circuit imperfections. Efficiency of the circuit is practically 80% in the range 1–100 kΩ, the consumption of the control circuitry not being taken into account.

When several modes are mixed, experimental results show that the power harvested with the Standard circuit remains smaller than with the SECE circuit, but the power ratio is weaker than in the case of harmonic vibrations.

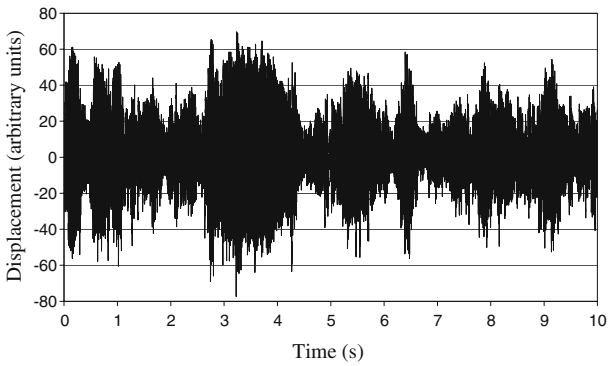

Fig. 11 Random displacement as a function of time

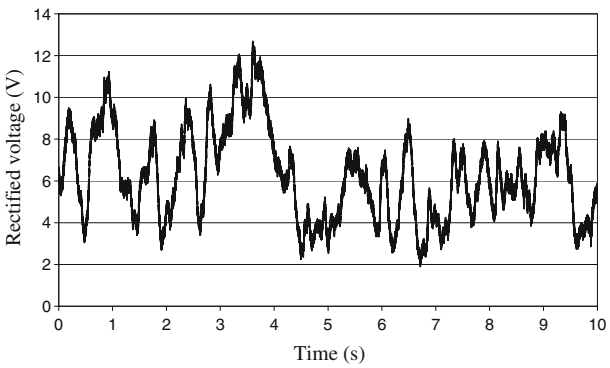

Fig. 13 Rectified voltage V_R as a function of time with the Standard interface and R_L=22 kΩ

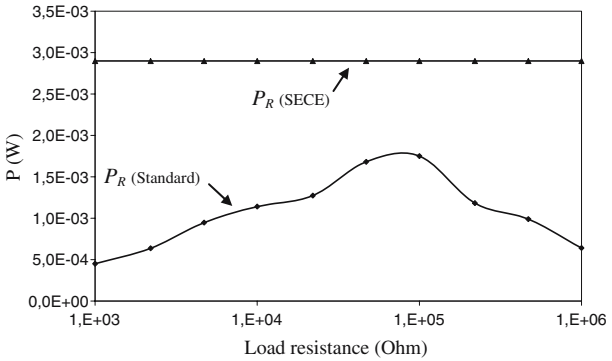

Fig. 14 Average powers as a function of the load resistance, PEG driven by a random force in the [10 Hz, 2 kHz] band

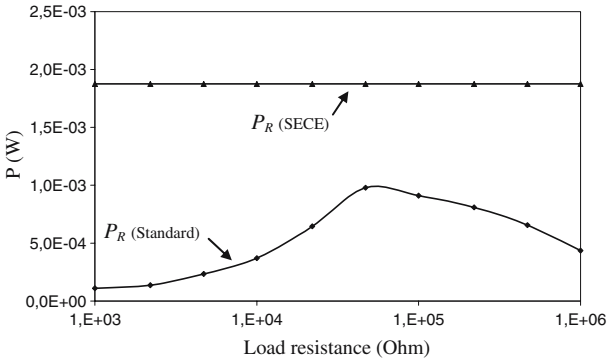

Fig. 16 Average powers as a function of the load resistance, PEG driven by a random force in the [10 Hz, 150 Hz] band

Figure 10 shows for instance a case in which the maximum power reached with the Standard interface is of 1.63 mW, whereas the input power of the SECE interface is of 2.76 mW: the power gain is here 1.7 only. In some cases, the SECE technique may harvest powers lower than the standard technique: for instance, if the PEG vibration is composed of a low-frequency mode with large amplitude mixed with a high-frequency mode with very weak amplitude. This drawback could be solved by selecting the right triggering times for extracting the electrical charge stored on the piezoelectric element, instead of triggering on each displacement extrema. In other words, effectiveness of the SECE technique could be improved by a "smart" choice among the local extrema of mechanical displacement (or among the local extrema of the piezoelectric voltage) for triggering the charge extraction process.

4 Broadband, random vibrations

The PEG cantilever steel beam is subjected to a random force generated by an electromagnet powered by a HP35665A random noise generator through a power amplifier. A low-pass filter is interleaved between the random noise generator and the power amplifier for limiting the frequency band. An image of the random mechanical displacement measured with a piezoelectric insert bonded on the PEG cantilever beam near the clamped end is shown on Fig. 11 for a 20 Hz–2 kHz frequency band. The corresponding displacement spectrum plotted on Fig. 12 reveals the mechanical filtering of the PEG mechanical part: the mechanical vibration is mainly composed of the three bending modes of the cantilever steel beam, respectively at 56, 334 and 915 Hz. The rectified voltage shape recorded in the case of the Standard power optimization technique is shown on Fig. 13. This plot gives an idea of the dynamic response required on the DC–DC power converter for a complete implementation of the Standard technique.

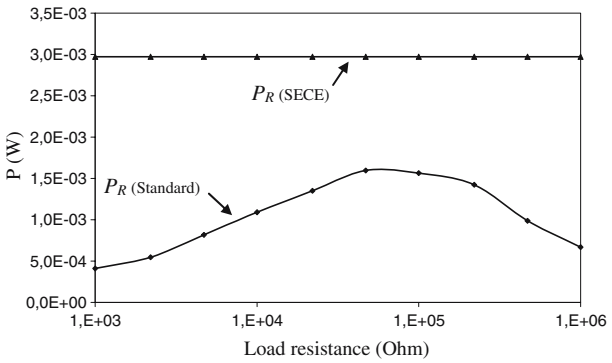

Fig. 15 Average powers as a function of the load resistance, PEG driven by a random force in the [10 Hz, 500 Hz] band

The average harvested powers are calculated from a 200 s recording of the instantaneous powers: there is a good repeatability of measurements on this temporal horizon. The results presented on Figs. 14, 15 and 16 are measured with random driving forces on different frequency bands. First, the frequency band of the driving force includes the three modes. The power harvested with the Standard technique reaches 1.75 mW for a 100 kΩ matching load resistance. In same operating conditions, the power harvested with the SECE technique is 2.9 mW. Then, the frequency band of the random driving force is restricted to modes 1 and 2. Powers harvested by the Standard and the SECE techniques reach respectively 1.6 mW (R_L=47 kΩ) and 2.97 mW. Finally, the frequency band is restricted so that the random force reveals the first bending mode only. In this case, the maximum power harvested by the Standard technique is 0.98 mW for an optimal load resistance R_L=47 kΩ, and the SECE power is 1.9 mW. Comparisons of the Standard power plots on Figs. 16 and 7 reveal some behaviour differences between harmonic and random operation for the first mode: the curve shapes are slightly different and the matching load resistances are not exactly the same. These differences are mainly due to the dynamic effect of the smoothing capacitor C_R on the V_R voltage variations. According to these plots, the SECE technique roughly

increase the harvested power by a factor 2 in random operation (mode 1 only), whereas the improvement factor is 3 in harmonic operation.

5 Conclusion

Theoretical and experimental results presented in this paper show that the both techniques, "Standard" and "SECE", allows to effectively harvesting energy from broadband, random vibrations using piezoelectric materials. Comparison between the Standard power optimization technique and the so called "Synchronized Electric Charge Extraction" technique exhibit several advantages of this last one. First, there is no need for load impedance adaptation. This property represents a great advantage because find and pursuing the load resistance value optimizing the Standard technique power may be relatively complicated in the case of broadband, random vibrations. Another advantage brought by the SECE technique is that the harvested power is increased by a factor up to 400% compared to the power of the Standard technique. Moreover, practical implementation of the SECE technique is much simpler than in the case of the Standard technique. Ongoing works aim at improving the efficiency of electronic circuits for both techniques in order to make comparisons of completely self-powered devices. Another part of these research works is focused on the development of smart strategies for selecting the right mechanical displacement extrema as triggering instants for electric charge extraction, in order to improve the broadband performances of this new technique.

Reference

1. S.W. Arms, C.P. Townsend, D.L. Churchill, J.H. Galbreath, S.W. Mundell, in *Proceedings of SPIE Smart Structures and Materials 2005*, ed. By V.K. Varadan (SPIE, Bellingham, 2005), vol. 5763, p. 267
2. A. Badel, E. Lefeuvre, C. Richard, D. Guyomar, J. Intell. Mater. Syst. Struct. **16**(10), 889 (2005)
3. D. Guyomar, A. Badel, E. Lefeuvre, C. Richard, IEEE Trans. Ultrason. Ferroelectr. Freq. Control **52**, 584 (2005)
4. E. Lefeuvre, A. Badel, C. Richard, D. Guyomar, J. Intell. Mater. Syst. Struct. **16**(10), 865 (2005)
5. E. Lefeuvre, A. Badel, C. Richard, D. Guyomar, Sens. Actuators, A, Phys. **126**(2), 405 (2006)
6. G.K. Ottman, H.F. Hofmann, G.A. Lesieutre, IEEE Trans. Power Electron. **18**, 696 (2003)
7. G.K. Ottman, H.F. Hofmann, A.C. Bhatt, G.A. Lesieutre, IEEE Trans. Power Electron. **17**, 669 (2002)
8. S. Roundy, E.S. Leland, J. Baker, E. Carleton, E. Reilly, E. Lai, B. Otis, J. M. Rabaey, V. Sundararajan, IEEE Pervasive Computing **4**(1), 28 (2005)
9. C.-N. Xu, M. Akiyama, K. Nonaka, T. Watanabe, IEEE Trans. Ultrason. Ferroelectr. Freq. Control **45**, 1065 (1998)